NUMERICAL MODELING OF FLOW AND MIXING OF SINGLE AND INTERACTING SWIRLING CO-ANNULAR JETS

Robert Szasz, Laszlo Fuchs
Department of Heat and Power Engineering
Lund Institute of Technology
Ole Romersv. 1, Lund 22100, Sweden
szrobi@mail.vok.lth.se, Laszlo.Fuchs@vok.lth.se

ABSTRACT

We consider the computation of the flow and mixing generated by a single or multiple co-annular swirling jets. The geometry of the burner that produces the jets is typical for a gas turbine burner. We consider both single and multiple, interacting burners. In addition to studying the turbulent flow field, we also consider the turbulent mixing of a passive scalar, injected to emulate fuel injection. In all the studies we use Large Eddy Simulations, assuming isothermal and incompressible flow. The confinement of the jets leads to larger internal re-circulating zones as compared to the corresponding free jet. Co- and counter rotation of the flow in the burners affect largely the flow and the mixing process. In addition, new modes of flow instability can be observed when multiple burners are considered.

INTRODUCTION

The increasing demands on low pollutant emission levels (especially concerning NO_x emissions) lead to the development of new methods in gas turbine technology. Such methods are for example the lean premixed and lean prevaporized premixed combustion methods. However, under these conditions, special care has to be taken to assure flame stability. A common way to stabilize the flame is the use of swirling jets. At sufficiently high swirl level an internal recirculation zone is formed and the recirculating hot gases will ignite the fresh mixture.

Swirling jets are characterized by a higher level of turbulence due mainly to the additional component of the shear (Naughton et al.,1997). The increased turbulence levels and entrainment enhances mixing in the case of swirling jets. In addition, the increased residence time contributes to a better mixing (cf. Naughton et al.(1997)). Another source of higher turbulence levels is the presence of centrifugal instabilities. Different modes of axi- and asymmetric instabilities due to swirl were studied experimentally by Panda and McLaughlin (1994) and more recently by Loiseleux and Chomaz (2003). These instabilities may lead to the formation of an internal recirculation zone (vortex breakdown). Different types of vortex breakdown were studied experimentally and categorized by Sarpkaya (1970) and by Billant et al. (1998). A recent review covering both experimental and numerical works dedicated to vortex breakdown is made by Lucca-Negro and O'Doherty (2001). Early numerical solutions of the Navier-Stokes equations for swirling flows were obtained with models based on Reynolds-averaging of the equations. However, Nejad (1989) demonstrated that $k-\epsilon$ based models require further modifications to accurately handle swirling cases. Ribeiro and Whitelaw (1980) concluded that Reynolds-stress closures cannot handle the strong anisotropy present in swirling flows. Recent computations (Repp et al., 2002) of the TECFLAM burner showed that the main features of the flow field can be predicted by Reynolds Stress Modeling, however the spreading rate of the central recirculation zone is overestimated. Due to these difficulties, numerical studies based on Large Eddy Simulation have been carried out in recent years (cf. Menon et al., (2001) and Sankaran and Menon, (2001)).

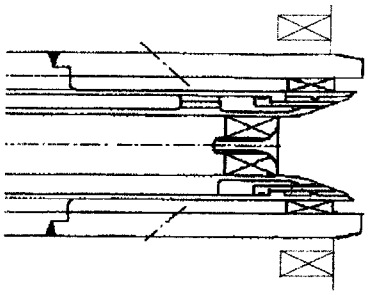

Figure 1: The geometry of the burner

The present paper focuses on the numerical study of the flow field generated by single and interacting co-annular swirling jets (burners). A sensitivity study (Szasz et al., 2001) made for the geometry but only with a single burner, revealed that one of the most important factors influencing the flow field is the confinement of the swirling jets by the combustion chamber. Gas turbine combustion chamber is of annular type with multiple interacting burners. There are only a few of such studies in the literature, a recent experimental work is made by Cai et al. (2002) involving an array of 3x3 burners. Both co- and counter-rotating configurations were evaluated. Here the single burner case is compared with results obtained with multiple burners. First, the geometry will be described followed by the numerical methods used in the computations. The results will show the influence of the neighboring jets on the flow field, especially on the size and shape of the internal recirculation zone and the turbulent mixing of a passive scalar.

PROBLEM DESCRIPTION

The considered geometry is typical for a gas turbine burner and is depicted schematically in Figure 1. Three co-axial swirling jets are entering the combustion chamber, providing 8%, 17% and 75% of the total mass flux, respectively. The swirlers' vanes have angles of 45^0, 38^0 and 52^0. In the computations the burner is approximated with the geometry presented in Figure 2. As can be seen in the figure the three inlets are not co-planar.

In the computations all lengths have been non-dimensionalized by the outer diameter of the outer swirler.

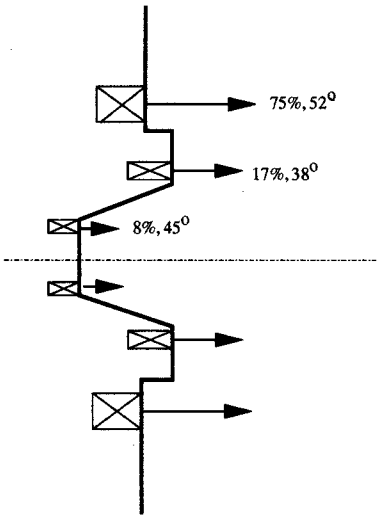

Figure 2: The geometry used in the computations

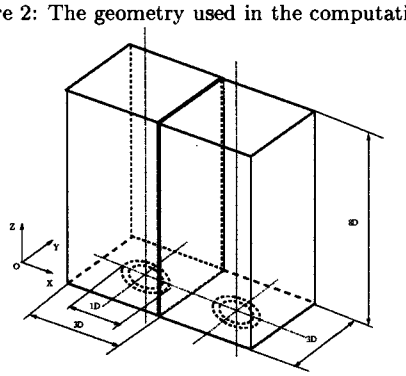

Figure 3: The geometry of the combustion chamber

The combustion chamber corresponding to one burner has a rectangular cross-section of 3x3 diameters, and a length of 8 diameters. Figure 3 shows the dimensions of the computational domain and the coordinate system used herein.

NUMERICAL METHODS

The flow is considered to be incompressible and isothermal. We also consider the mixing of two passive scalars, having Schmidt numbers (Sc) 1.0 and 0.2, respectively. The scalars, representing the fuel, are injected through the middle swirler. The equations describing the flowfield are:

$$u_{i,i} = 0 \tag{1}$$

$$\rho u_{i,t} + \rho u_j u_{i,j} = -p_{,i} + \frac{1}{Re}(u_{i,j})_{,j} \tag{2}$$

$$c_{i,t} + u_j c_{i,j} = \frac{1}{Pe}(c_{i,j})_{,j} \tag{3}$$

Where $Pe = ReSc$.

Turbulence is accounted for by Large Eddy Simulation (LES), which is able to cope both with the strong anisotropy and streamline curvature present in swirling flows. Additionally, it can handle the unsteadiness of the flow field, which is required if low frequency motion is to be studied. The Sub-Grid Scale (SGS) terms are not modeled explicitly. Thus, the truncation errors account for the dissipative effect of the SGS-terms. This approach proved to be accurate if the grid resolution is high enough (Olsson and Fuchs,1996).

The equations are discretized using a fourth order finite difference scheme except the convective terms, which are discretized with a third order upwind scheme. Second order implicit discretization is used for integration of the equations in time. The grid is Cartesian and staggered, with a possibility to have local refinements. In the computations approximately 1.2 million cells have been used for each burner.

In order to maintain the computational time on reasonable levels the code was parallelized based on the Message Passing Interface (MPI) library. Each processor was computing a part of the computational domain corresponding to a single burner. In this way a good speed-up could be achieved, the time needed for communications is only about 4% of the total computational time.

The Reynolds number in all computations was set to 20000. The axial component of the inlet velocity was computed to assure the mass flux distribution presented in the previous section. The tangential components were computed based on the assumption that the ratio of the tangential and axial velocity components is determined by the angle of the swirler vane. The radial components of the inlet velocity were assumed to be zero. All velocity components were constant in radial direction for a given swirler. At the outlet flux-conserving zero gradient boundary condition was imposed. No-slip conditions are applied at the solid, side-walls.

RESULTS AND DISCUSSIONS

Effects on the shape and size of the internal recirculation zones

In a previous study (Szasz et al., 2001) it was observed that confinement influences strongly the size and shape of the internal recirculation zone (IRZ). With decreasing cross section of the combustion chamber the IRZ became stronger. It was expected that having two neighboring burners in the combustion chamber the IRZ will change significantly.

In Figure 4 the isosurface of zero mean axial velocity is presented for three of the considered configurations. This isosurface can be regarded as the limit of the internal recirculation zone. Isocontours of the axial velocity component in longitudinal cross sections for the same configurations are presented in Figure 5. In the figure dashed lines represent negative values of the axial velocity.

In the case of a single burner (see Figure 4(a)) one can observe conical shaped, elongated IRZ. As one can see in Figure 5(a), the jets are attached to the combustion chamber walls already at around 1.2 diameters downstream of the inlet and remain attached further downstream. As a result, the central recirculation zone is present (even if it has a small diameter), at distances as large as 8 diameters downstream. Additionally, another vortex, due to the corners of the combustion chamber is clearly visible.

When two burners are present, the structure of the flow field becomes more complicated, both in the co- (Figure 4(b)) and counter-rotating (Figure 4(c)) cases. The vortex breakdown bubbles became shorter, their length is approximately 4 diameters in both cases. Even if their size is approximately the same, significant qualitative differences are observed between the two cases. When the jets are rotating in the same directions, the axis of the IRZ is tilted in the direction of the inlet swirl, showing that a global swirl is generated having the same direction as the individual swirlers. In the counter-rotating case, however, the axis

of the IRZs remain vertical almost all the length of the recirculation zone. These two cases will be compared in more details in the next subsection.

Increasing the number of burners to 3 (not shown here) leads to a further decrease of the size of the internal recirculation zone, the middle burner having the smallest one (length of about 2.5 diameters), while the other two burners have recirculation zones of approximately 3.5 diameters.

Co- vs. counter-rotating configuration

We consider first the flow field qualitatively. This has been done by considering the motion of tracer particles in the flow field. The tracer particles have been released at corresponding places, when multiple burners are present. In the following we describe these results, though no figures are shown. At half a diameter downstream (Z=0.50), there are some important differences. In the case of co-rotating burners, one can notice the collaboration of the two burners in creating a global circular motion along the walls, while at the interface of the two burners, as it is expected, the circular motion is diminishing due to the opposite sign of the tangential velocity component. In the counter-rotating case, however, the tangential velocities at the interface have the same sign and one can see the two individual swirls created by the burners. Additionally, at this axial distance, one can notice in both cases the presence of the outer recirculation zone. Further downstream, one can observe the presence of the strong recirculation zones. Additionally, the differences described previously are even more clear. At about 3.0 diameters from the burner outlet, the strength of the recirculation zones decreases. However, in the counter-rotating case the swirl is much stronger than in the co-rotating case. This is in agreement with the observations of Cai et al. (2002). They observed experimentally in the case of a matrix of 3x3 burners that in a counter-rotating configuration the swirl created by individual burners is visible longer downstream than in the co-rotating case. One can also observe the displacement of the axis of the individual vortices for the co-rotating case due to the generated global swirl. The corresponding counter-swirling case is symmetric, and only a displacement of the axis of both vortices towards the bottom part of the burners is noticeable.

The radial distribution of the mean axial and tangential velocity components, at one diameter downstream is depicted in Figure 6(a) and Figure 6(b). The axial flux coming from the two counter-rotating burners maintain a symmetry that cannot be seen in the corresponding co-rotating case. Further downstream, however, the interaction between the burners can be seen in the tangential profiles as well.

Interaction between burners

A measure of the interaction between the two burners is defined to be the correlation of the axial velocity component at corresponding axial positions along the axis of the two burners.

$$c(z) = \frac{\overline{w_1(z)w_2(z)}}{\overline{w_1(z)w_1(z)}} \qquad (4)$$

where $w_1(z)$ is the axial velocity at position z on the symmetry axis of the first burner and $w_2(z)$ is the axial velocity at the same axial position on the symmetry axis of the second burner. Figure 7 shows the comparison of these correlations for the co- and counter-rotating cases. As one can observe in both cases there is a strong correlation at around

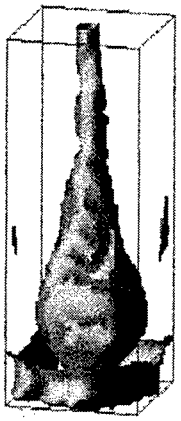

(a) One burner

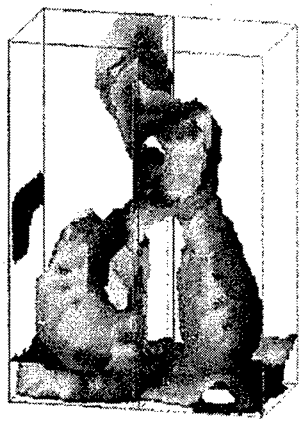

(b) Two burners, co-rotating

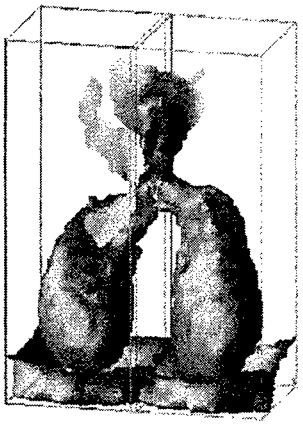

(c) Two burners, counter-rotating

Figure 4: Comparison of the separation bubble for different configurations

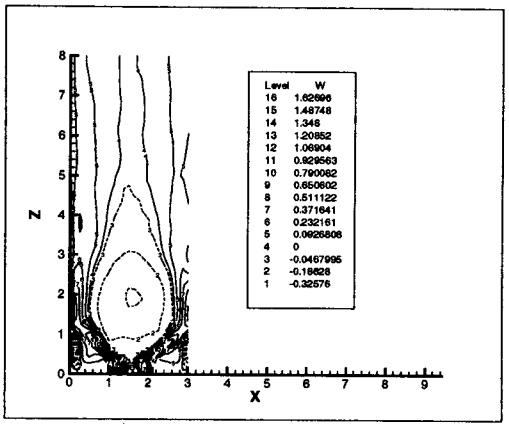

(a) One burner

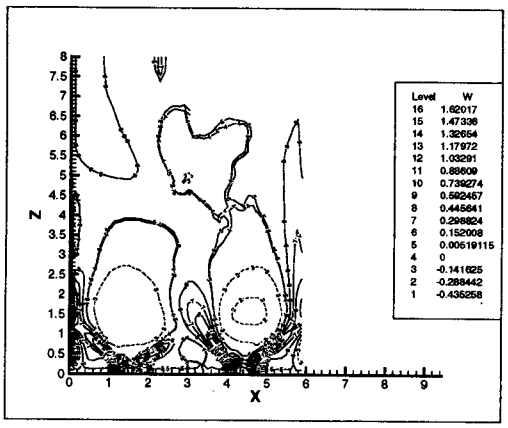

(b) Two burners, co-rotating

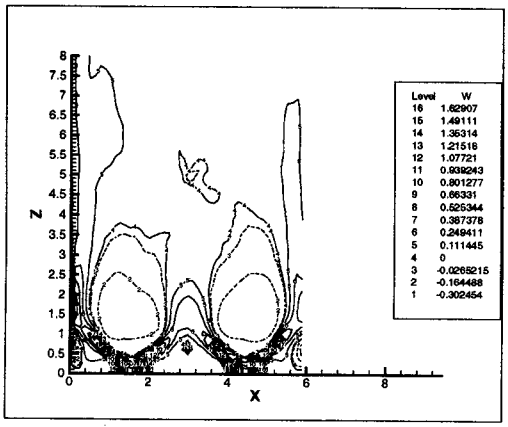

(c) Two burners, counter-rotating

Figure 5: Iso-contours of the mean axial velocity component in longitudinal cross-sections for different configurations. Dashed lines represent negative velocity.

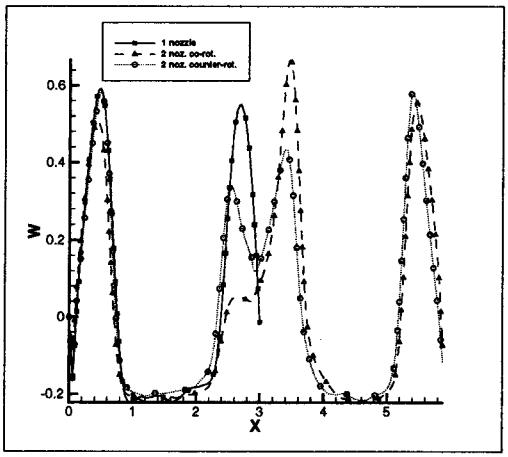

(a)

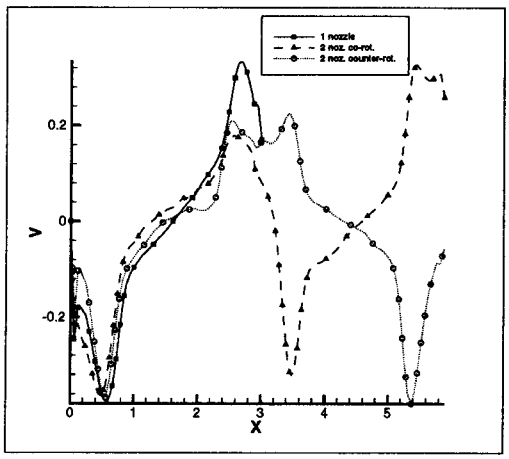

(b)

Figure 6: Mean axial velocity (a) and tangential velocity (b) along a radial line at 1.0 diameter downstream

2 diameters downstream of the inlet. This can be explained by the fact that at this axial position the shear layer of the swirling jets of the two burners are merged. Further downstream the diameter of the recirculation bubble decreases and as a consequence there is less interaction between the jets.

Low frequency oscillations

One of the crucial problem in swirling flows is the possible appearance of low-frequency oscillations in the flow-field. These oscillations may enter in resonance with the solid structure or may give rise to thermo-acoustic oscillations. None of these phenomena is desirable in gas turbine applications.

Data was collected from 8 monitoring points per burner, arranged symmetrically around the axis, in planes situated at two axial positions, 0.75 and 4.5 diameters, respectively. Fourier analysis of the resulting velocity history revealed the presence of low-frequency motions with a non-dimensionalized frequency of 0.2. For example, Figure 8 shows the Fourier spectrum of the axial component of the velocity in a point situated at 0.75 diameters from the inlet,

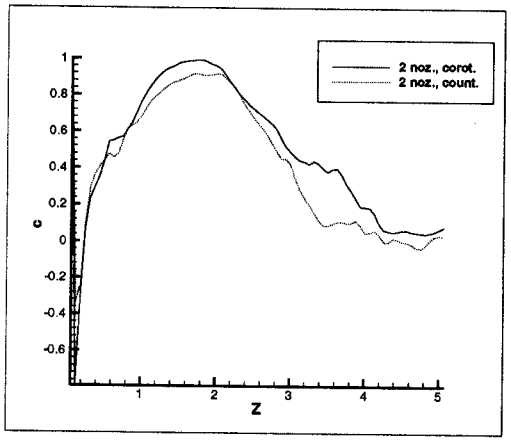

Figure 7: Correlation between the axial velocity component along the centerline of the two burners

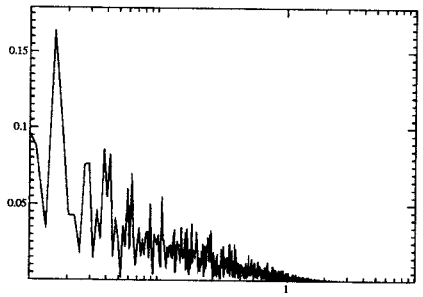

Figure 8: Frequency spectra of the axial velocity component

between the two burners, at 1.0 diameter from the axis of the second burner. Similar results are obtained also for the other monitoring points.

To determine which kind of motion produces the high amplitude at 0.2, time history of the axial velocity component is plotted in Figure 9 along a radial line positioned at 3.0 diameters downstream from the inlet. In the figure the iso-contour of zero axial velocity is plotted to visualize the motion of the IRZ, the vertical axis being the time. The left part of the figure presents the time evolution along a line parallel to the X direction, while the right side represents the evolution along a line in Y direction (for the coordinate system shown in Figure 3). As one can observe, periodical motions are clearly visible in the Y direction, while in the X direction the patterns are more symmetric. Figure 10 presents in a similar way the evolution of the axial velocity along the symmetry axis of the second burner. Again, periodical displacement of the IRZ is observed. Thus, the low frequency motion consists of oscillations parallel to the X- and Z-directions, respectively.

Mixing

Consider the mixing of two passive scalars having different molecular diffusivities. There have been arguments in the literature that for large Reynolds numbers, the turbulent mixing (assuming it is large enough) is independent of the Schmidt number. In combustion of hydrocarbons the different species have different molecular diffusivity. Hydrogen has smaller Sc than unity while oxygen has Sc about unity and the fuel usually larger than unity. Assuming unity

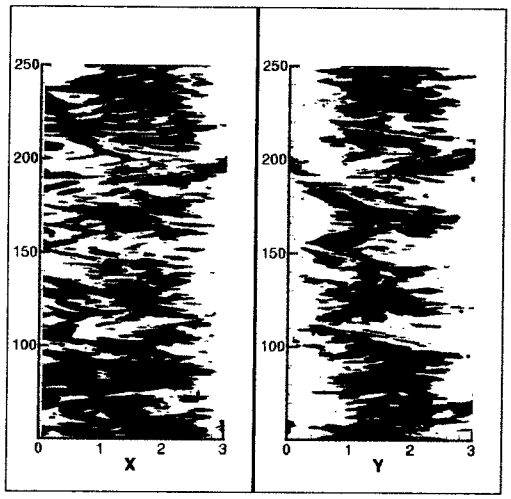

Figure 9: Time history of the axial velocity component along a radial line situated at 3.0 diameter downstream from the inlet

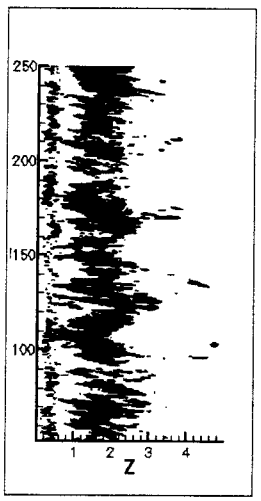

Figure 10: Time history of the axial velocity component along the symmetry axis of the second burner

Lewis number (and by this same Sc for all species) simplifies considerably the treatment of the reacting flow problem. However, as shown in Figure 11 there is a clear effect of "differential diffusion". The Sc number effect is present when one finds large-scale structures that support large shear. In such cases the turbulent mixing cannot counteract the effect of advection-diffusion at the shear layer. This is the case in a typical gas turbine burner, where the shear layers are created for enhancing liquid fuel break-up and mixing of the vaporized fuel. This effect of differential diffusion is also found when multiple burners interact. Figure 12 shows the variation of the axial velocity along a line normal to the two symmetry axis of the burners, situated at 3.0 diameters downstream. The center of the burners is situated at the positions marked with 1.5 and 4.5 on the horizontal axis. One can observe a strong asymmetry of the axial velocity profile in the co-rotating case compared with the counter-rotating burners. This is due to the vortex generated further downstream which decreases the axial flux in the region of the combustion chamber corresponding to the left burner. Due to this asymmetry in the velocity field, there is an asymmetry in the scalar concentration field as well. In Figure 13, depicting the scalar concentration along the same line, one

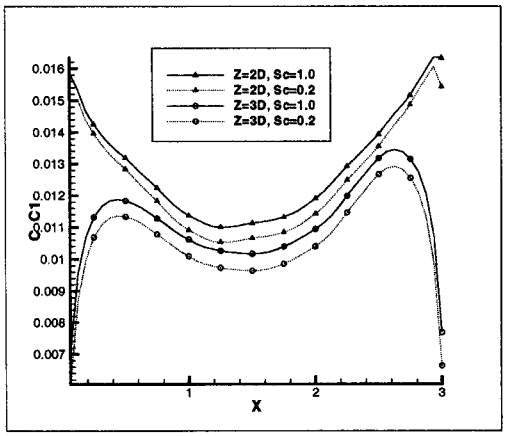

Figure 11: Scalar concentrations along radial lines at Z=2D and Z=3D

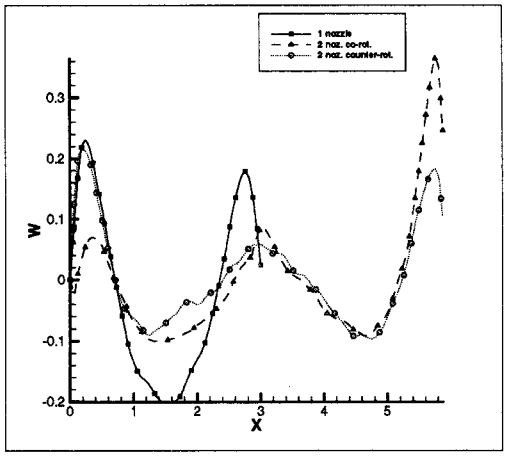

Figure 12: Axial velocity along a radial line at 3.00 D downstream from the inlet

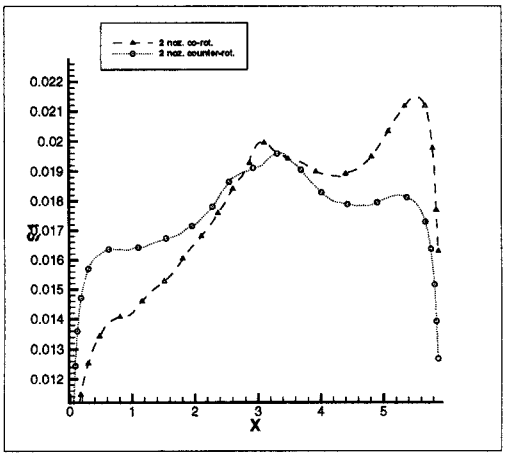

Figure 13: Scalar concentration along a radial line at 3.00 D downstream from the inlet

can notice the decreased concentration levels in the left side of the combustion chamber for the co-rotating case, while the counter-rotating case presents more symmetric values. This shows that a counter-rotating configuration may be better from a mixing point of view.

CONCLUSIONS

The LES shows clearly that detailed analysis of a single burner does not reflect the behavior of the burners in a gas turbine chamber. The effects of the walls of the chamber determine also the stability of the single burner flow. In the presence of multiple burners, co- and counter-rotation has important effect on the stability and the separation bubble (used for flame holding). In addition, we have found that the Schmidt number has a clear importance in these burner geometries. Thus, the highly simplifying assumption of unity Lewis number is questionable.

ACKNOWLEDGMENTS

The financial support from the Swedish Research Council (VR) is greatly acknowledged. Additionally, the authors would like to acknowledge the computational time offered by the super-computing center at Lund University (LUNARC) and the Swedish National Supercomputer Center (NSC).

REFERENCES

Billant, P., Chomaz, J.M., and Huerre, P., 1998, "Experimental study of vortex breakdown in swirling jets", *J.Fluid Mech.*, Vol.376, pp.183-219.

Cai, J., Jeng, S.M., and Tacina, R., 2002, "Multi-swirler aerodynamics: comparison of different configurations", *Proceedings of ASME Turbo Expo 2002, June 3-6, 2002, Amsterdam, The Netherlands.*

Loiseleux, T., and Chomaz, J.M., 2003, "Breaking of rotational symmetry in a swirling jet experiment", *Phys.Fluids*, Vol.15(2), pp.511-523.

Lucca-Negro, O., and O'Doherty, T., 2001, "Vortex breakdown: a review", *Prog. Energy and Combustion Science*, Vol.27, pp.533-552.

Menon, S., Sankaran, V., and Stone,C., 2001, "Dynamics of Swirling Premixed and Spray Flames", *AIAA paper 2001-1092.*

Naughton, J.W., Cattafesta, L.N., and Settles,G.S., 1997, "An experimental study of compressible turbulent mixing enhancement in swirling jets",*J.Fluid Mech.*, Vol.330, pp.271-305.

Nejad, A.S., Vanka, S.P., Favaloro, S.C., Samimy, M., Langenfeld, C., 1989, "Application of Laser Velocimetry for Characterization of Confined Swirling Flow", *J. of Engineering for Gas Turbines and Power*, Vol.111, pp.36-45.

Olsson,M., and Fuchs,L., 1996, "Large Eddy Simulation of the Proximal Region of a Spatially Developing Circular Jet", *Phys.Fluids*, Vol.8, pp.2125-2137

Panda, J., and McLaughlin, D.K., 1994, "Experiments on the instabilities of a swirling jet", *Phys.Fluids*, Vol.6(1), pp.263-276.

Repp, S., Sadiki, A., Schneider, C., Hinz, A., Landenfeld, T., Janicka, J., 2002, "Prediction of swirling confined diffusion flame with a Monte Carlo and a presumed-PDF model", *Intl.J. of Heat and Mass Transfer*, Vol.45, pp.1271-1285.

Ribeiro, M.M., Whitelaw, J.H., 1980, "Coaxial jets with and without swirl", *J.Fluid Mech.*, Vol.96, pp.769-795.

Sankaran, V., and Menon, S., 2001, "LES of spray combustion in compressible high Reynolds number swirling flows", *Proceedings of Turbulence and Shear Flow Phenomena, Second Symposium, Stockholm*, Vol.II, pp.303-308.

Sarpkaya, T., 1970, "On stationary and traveling vortex breakdowns", *J.Fluid Mech.*, Vol.41, pp.727-736.

Szasz, R.Z., Caraeni, D.A., Fuchs, L., 2001, "Study of mixing in swirling turbulent jets", *Proceedings of IUTAM Symposium on Turbulent Mixing and Combustion, Kingston, ON, Canada.*